Journal of Engineering Science and Technology
Special Issue on SU18, February (2019) 273 - 285

OPTIMAL PERFORMANCES OF SINGLE-PHASE FIELD EXCITATION FLUX-SWITCHING MACHINE USING SEGMENTAL ROTOR AND NON-OVERLAP WINDINGS

MOHD FAIROZ OMAR*, ERWAN SULAIMAN, HASSAN ALI SOOMRO, MOHD ASYRAF ABDUL RAHIM, JAUDAH ABD RANI

Electrical Power Engineering Department, Faculty of Electrical and Electronic Engineering, Universiti Tun Hussein Onn Malaysia,
86400 Parit Raja, Johor, Malaysia
*Corresponding Author: fairoz.omar@yahoo.com

Abstract

Field Excitation Flux Switching Machines (FEFSMs) in which, their torque performance generated by the interaction between armature and Field Excitation (FE) coils have been widely designed and developed for various applications. In this regard, FEFSM with the salient rotor is considered the most suitable candidate for high-speed applications because of their advantages of flux controllability, and robust due to a single piece of rotor structure. However, the salient rotor structure is found to produce low torque performance due to the longer flux path in stator and rotor yielding weak flux linkage. In this paper, a new FEFSM using a segmental rotor with advantages of shorter flux path is proposed. The segmental rotor has improved the flux flow and reduced flux leakage to produce higher torque. For comparison, both FEFSMs with salient and segmental rotors have been designed using JMAG Designer version 15 and the investigation process is done via 2D-FEA. As a result, the magnetic flux of the segmental rotor design is 11 times higher than the salient rotor structure mainly due to shorter magnetic flux linkage between two stator teeth and a single rotor segment. In addition, the optimization process of the proposed motor has been conducted by using deterministic optimization technique. The flux linkage, torque and power for the proposed motors have achieved optimum performances of 0.0714 Wb, 1.65 Nm, and 398.6 W, respectively. In conclusion, the proposed motor is considered as the best single-phase FEFSM candidates, with 85.4% and 43.6% improvement of torque and power, respectively.

Keywords: Field excitation flux-switching machine, Non-overlap winding Optimization, Segmental rotor, Single-phase.

1. Introduction

Flux-Switching Motors (FSMs), an unfamiliar class of electric motor originated from the blend of switched reluctance motor and inductor alternator have been mostly designed as part of Hybrid Electric Vehicles (HEVs) drive system due to their high torque and high power density capabilities [1]. The FSMs have generally been classified into three major groups of permanent magnet FSM (PMFSM), field excitation FSM (FEFSM), and hybrid excitation FSM (HEFSM) initiated from their fundamental flux sources [2]. Structurally, most of the permanent magnet (PM) excitation located on the stator of traditional PMFSM can be viably supplanted by DC field excitation coil (FEC) to form FEFSM [3], while HEFSM combines both PM and FEC as its main flux source [4].

As such, the FEFSM is a type of salient rotor machine with a novel topology with prodigious magnetic flux controllability. The idea of the FEFSM includes changing the polarity of the flux linking the armature winding, as for the rotor rotation [5]. Consequently, the FEFSM offers advantages of the magnet-less motor, low starting torque, low cost and simple structure suitable for various performances. Numerous topologies of FEFSM have been considered and the machine's reliability has moreover, been tested in an assortment of applications requiring high torque and high power density [5, 6]. Furthermore, coil configuration and winding polarity in FEFSMs have affected motor performances, especially on copper loss and efficiency. Suleiman et al. [7, 8] explained that as an example, FEFSMs with single and dual polarity FEC have been discussed. The advantages of FEFSM with single polarity FEC are low copper loss due to less capacity of FEC as well as less flux leakage when compared with dual FEC windings. Additionally, based on studies by Tang et al. [9], the field weakening capability of FEFSM is improved using toroidal FEC winding.

Figure 1 illustrates an example of three-phase 12S-5P [10] and single-phase 12S-6P [11] FEFSMs with salient rotor design. From Fig. 1(a), the motor consists of 6 armature slots, 6 FEC slots, and a single robust salient rotor in the middle. The introduced motor is suitable for industrial application variations such as electric vehicles due to the high torque performance of 320 Nm at a base speed of 800 rpm. Though their performances are well suited for high speed and torque applications, the overlap armature coil, and FEC windings give a significant impact of increased motor size due to higher copper usage and efficiency reduction due to copper losses increment.

In order to reduce the usage of copper, single-phase 12S-6P FEFSM with the salient rotor as illustrated in Fig. 1(b) is introduced. The motor consists of 4 armature coils winding, 4 FECs winding, and 6 poles of the salient rotor in the middle. The main advantage of this motor is less copper loss due to the FEC is wounded between two adjacent slots has reduced copper consumption and produced shorter end winding. However, a considerable distance between rotor poles is found to lead an extended magnetic flux path flowing from stator to the rotor and vice versa, producing a weak flux linkage as well as a low torque performance. In this research, a new single-phase FEFSM using a segmental rotor and non-overlap windings is proposed. The objectives of this paper are to design and analysis performances of new single-phase 12S-6P FEFSM using a segmental rotor and non-overlap winding thru JMAG designer version 15 and to optimize the performances of the proposed motor using deterministic optimization method. The proposed motor is expected to produce a short magnetic flux path, high magnetic flux linkage, and high output torque.

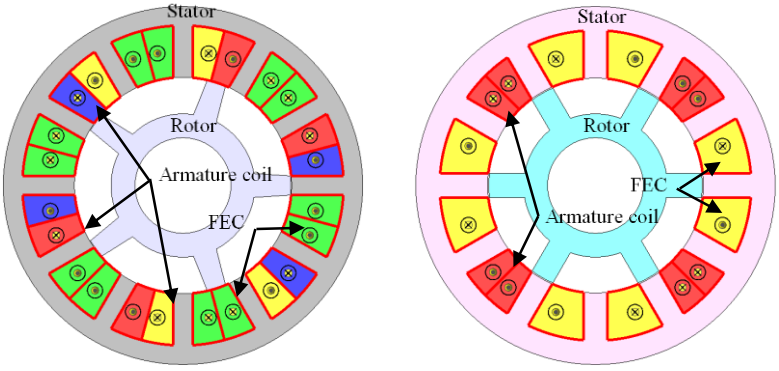

(a) 3-phase 12S-5P. **(b) Single-phase 12S-6P.**

Fig. 1. Example of FEFSM.

2. Preliminary Topology of FEFSM Machine Figure 2 demonstrates the initial design of single-phase 12S-6P FEFSM with 12 slots armature coils winding, 12 slots FECs winding and 6 segmental rotors with 26° rotor span. Obviously, all armature coils and FECs winding are placed alternately with non-overlap winding amongst each other and are set with a similar slot area of 47 mm^2 under 15° opening angle. The outer diameter of the rotor and stator are set to 44.5 mm and 75 mm, respectively. To ensure similar resulting flux profile of the armature coil winding, both FEC1 and FEC2 windings are set in the opposite direction between armature coil winding. In addition, comparison of FEFSM with segmental and salient rotors under the same stator configuration is conducted to verify the segmental rotor capability against FEFSM. In short, comparable stator tooth and stator yoke widths are expected to provide sufficient flux path, enables smooth flux linkage and less flux saturation.

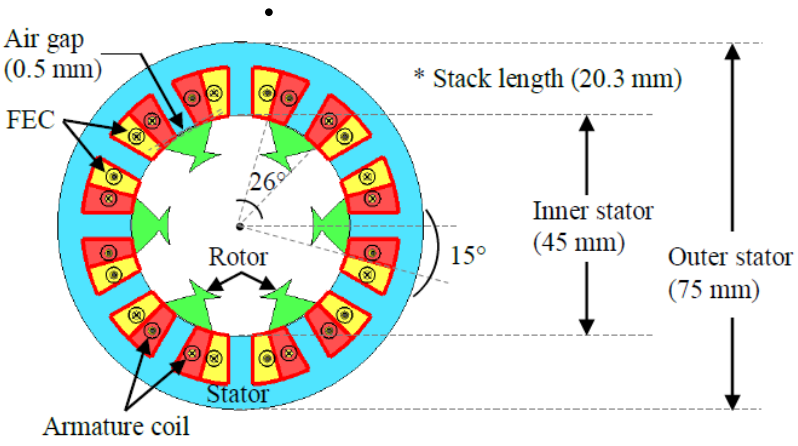

Fig. 2. Proposed structure of FEFSM using segmental rotor.

3. Design Optimization

In order to improve performances of torque and power, the refinement process is carried out by using a deterministic optimization technique. This method is performed by changing the design parameters of the motor, from one side to one part freely until the motor achieves the highest torque performance.

Morever, the deterministic optimization method is expected to solve the problem of back-emf disruption, unbalanced armature flux, and unsmooth FEC flux linkage.

Generally, there are seven parameters involved in the optimization process: rotor outer radius (R_1), segmental rotor span (R_2), segmental rotor high (R_3), armature slot high (A_1), armature slot width (A_2), FEC slot high (F_1), and FEC slot width (F_2) as illustrated in Fig. 3.

Furthermore, it should be noted in the optimization process, the following parameters need to be maintained as initial parameter: outer radius of stator (S_o), armature and field excitation number of turns (N_A and N_E), air gap (A_g) and current input of armature and field excitation (I_A and I_E).

Figure 4 shows the deterministic optimization method procedure of the proposed FEFSM using a segmental rotor. From the figure, each optimization cycle is divided into four stages involving rotor, armature slot, FEC slot and, performance comparison between optimized torque, T_{opt} and previous cycle torque, Tc_i. Stages 1 to 3 shows the optimization order according to the parts of the proposed motor.

To ensure the optimal torque is achieved, the comparison between T_{opt} and Tc_i in stage 4 is performed, in which, T_{opt} same as Tc_i, while if T_{opt} higher than Tc_i, stages 1 to 3 needs to be repeated.

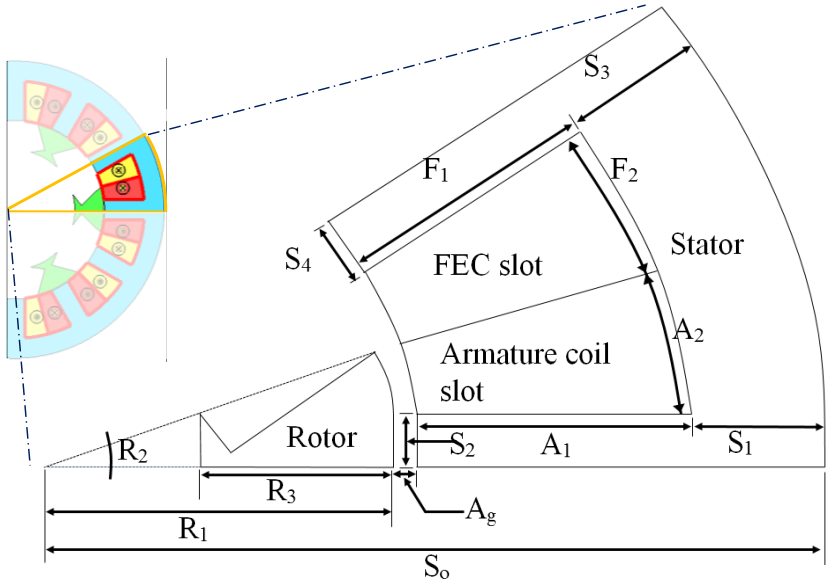

Fig. 3. Parameter sensitivities in optimization processes.

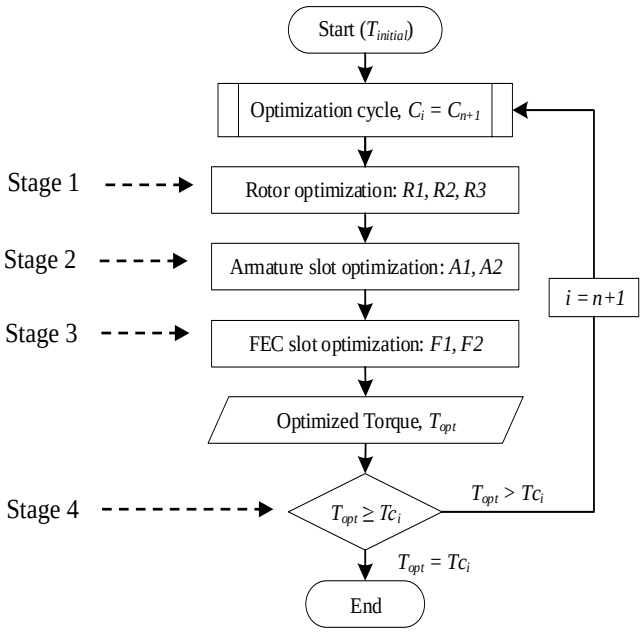

Fig. 4. Optimization procedure.

4. Performances of FEFSM using Segmental Rotor

This section discusses performances of proposed FEFSM using segmental rotor obtained from the preliminary design until the optimization process is completed. Figure 5 shows the flux profile at various FEC current density, J_E of both FEFSM with segmental and salient rotors. Obviously, the segmental rotor has produced the highest flux of 0.0412 Wb, 11 times higher than the salient rotor.

The significant difference in flux performance is due to magnetic flux route factors. In which, flux of salient rotor is linked between three stator teeth and two rotor teeth, while the flux of segmental rotor is linked through two stator teeth and one rotor segment as demonstrated in Fig. 6. In short, the segmental rotor structure has facilitated flux to flow in short magnetic path.

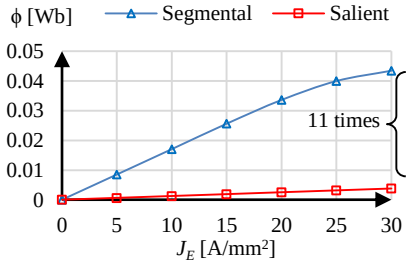

Fig. 5. Flux at various FE current density, J_E.

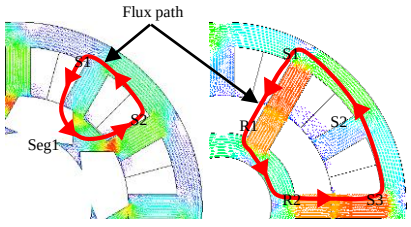

Fig. 6. Flux path, (a) segmental rotor, and (b) salient rotor.

4.1. Segmental rotor and stator ratio

The Split Ratio (*Sr*), is defined as the ratio of the outer rotor radius (R_1) with respect to the Outer Stator radius (S_o). The initial *Sr* of the single-phase FEFSM using segmental rotor is 0.593. The best split ratio is obtained by changing R_1 upward and downward for several cycles. Since the armature coil current, I_A and FEC current, I_E values need to be aligned throughout the optimization process, parameters such as *A1*, *A2*, *F1*, and *F2* must be changed to maintain the slot area of 47 mm^2. Table 1 and Fig. 7 show the torque performances based on outer rotor radius optimization and torque versus split ratio, respectively.

From Fig. 7, in the first cycle of optimization under the initial stage, the torque only increased by 0.02 Nm at a split ratio of 0.62. In the second cycle of optimization, the highest torque of 1.57 Nm is obtained when the split ratio is set to 0.593. While, in the third cycle, the highest torque of 1.61 Nm is achieved when the split ratio is set to 0.567. From the analysis, it is found that the ideal torque can be achieved by decreasing the *Sr* between parameters R_1 and S_o. In short, by lowering the *Sr*, the R_1 has decreased, while the parameter of stator yoke (S_1 and S_3) have increased and enable smooth flux linkage to produce higher torque.

Table 1. Torque performances based on outer rotor radius optimization.

R_1 (mm)	*Sr* (%)	1st cycle (Nm)	2nd cycle (Nm)	3rd cycle (Nm)
20.25	54.0	0.85	1.36	1.542
21.25	56.7	0.88	1.51	1.610
22.25	59.3	0.89	1.57	1.605
23.25	62.0	0.91	1.56	1.546
24.25	64.7	0.90	1.46	1.375
25.25	67.3	0.84	1.21	1.105
26.25	70.0	0.72	0.90	0.789

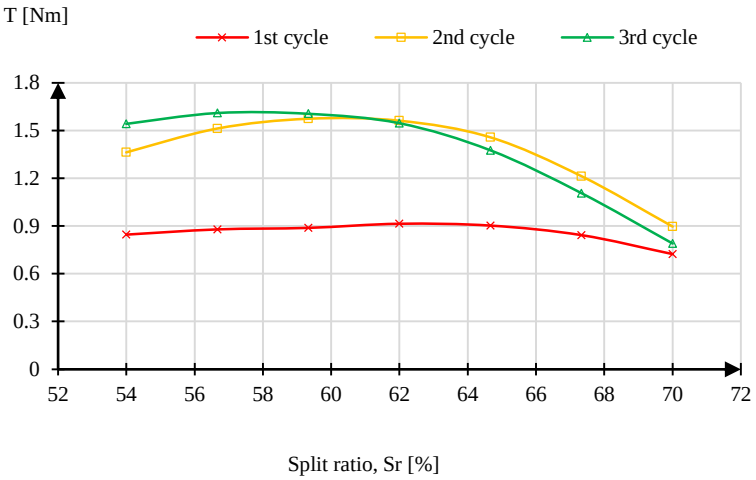

Fig. 7. Torque versus split ratio, *Sr*.

4.2. Segmental rotor span and high

In an effort to reduce the flux leakage and iron loss as well as to build more flux concentrating, segmental rotor span (R_2) and segmental rotor high (R_3) need to be refined. The preliminary parameter of R_2 is set to 15° while the refinement process is performed with altering R_2 from 15° to 28°, 18° to 28°, and 21° to 28° in the first cycle, second cycle, and third cycle, respectively by keeping all other parameters constant. Figure 8 demonstrates torque versus R_2 in three cycles of optimization. At the first cycle, the highest torque of 1.56 Nm, increased by 71.4% from the highest torque achieved in the first cycle of R_1 refinement. The highest torque of 1.59 Nm and 1.61 Nm have achieved in the second and third cycles, respectively were obtained when segmental rotor span is set to 25°.

Moreover, the result of R_3 optimization is depicted in Fig. 9. Optimization of R_3 was performed by changing the R_3 parameters from 5.25 mm to 13.25 mm in the first cycle, 4.25 mm to 12.25 mm in the second cycle, and 3.25 mm to 11.25 mm in the third cycle. The highest torque of 1.56 Nm, 1.60 Nm, and 1.61 Nm is obtained in first, second and third cycles, respectively. The highest torque produced in the first cycle presented R_3 of 8.25 mm slightly lower than the R_3 of 8.25 mm in the second and 7.25 mm in the third cycles. From the figure, the highest torque in each cycle has not much different. This occurred due to a lot of flux characteristics have been changed during the R_2 optimization process. Besides, in R_3 optimization, only the inner part of the motor is involved, in which, the stator structure remains unchanged.

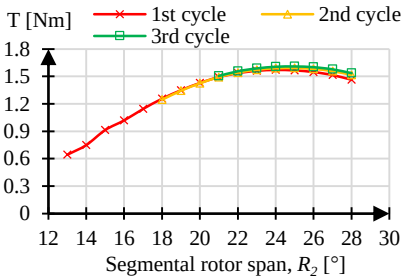

Fig. 8. Torque versus segmental rotor span, R_2.

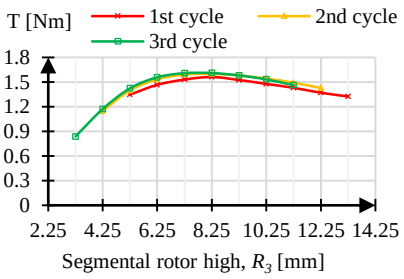

Fig. 9. Torque versus segmental rotor high, R_3.

4.3. Armature coil slot

Armature and FEC slots optimization are expected to improve the structure of the motor, as well as to improve the flux characteristics in both tooth and yoke of the stator. Furthermore, it should be noted that when parameters A_1 and F_1 are changed, armature coil and FEC stator width (A_2 and F_2), stator yoke (S_1 and S_3) and stator tooth width (S_2 and S_4) are changed to ensure similar armature slot area. Consequently, the highest torque achieved at the end of the optimization process is actually generated from the same supply value based on the number of turns obtained from fix FEC and armature coil slot areas. Figure 10 shows the torque characteristics against the armature slot high (A_1). From the figure, the highest torque of 1.56 Nm is obtained in the first cycle, while the highest torque of 1.60 Nm is achieved in second and third cycles. In the third cycle, the highest torque has been achieved when A_1 is set to 10.4 mm, while the corresponding parameters of A_2, S_1 and S_2 are 5.85 mm, 5.6 mm and 2.5 mm, respectively.

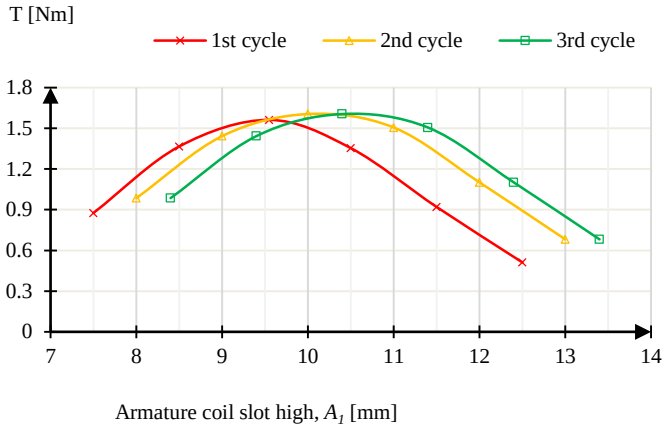

Fig. 10. Torque versus armature coil high, A_1.

4.4. FEC slot

Torque versus various FEC slot high (F_1) is illustrated in Fig. 11. For the armature slot high optimization, the final parameter F_1 has increased from 10 mm to 11.4 mm, while F_2 of 5.6 mm has decreased by 8.8% compared to the preliminary design. Besides, the S_4 parameter has expanded to 3 mm from 2.5 mm initially and thus, increasing the flux linkage to the rotor. From the figure, third cycle optimization shows the highest torque of 1.65 Nm, 9.3% higher compared to the torque in the second cycle. While in the first cycle, the highest torque of 1.56 Nm is achieved when F_1 is set to 9.55 mm.

Figure 12 illustrates three cycles of optimization to realise optimal torque by updating seven parameters of the proposed motor. From the figure, it is clear that the torque at the early stage of the first cycle has increased sharply from 0.91 Nm to 1.56 Nm through optimization of R_2. The torque of 1.56 Nm achieved at the end of the first cycle showed a 75.3% increase from the torque of the preliminary design. Then, in the second cycle torque has been increased to 1.6 Nm, and then slightly increased to 1.65 Nm, 85.4% higher than the preliminary torque performance during the optimization of F_1 and F_2 at the end of the third cycle. In short, the torque increases sharply in the early stages and then becomes constant, confirming the optimal parameters of the proposed motor as illustrated in Table 2.

Table 2. Initial and optimized design parameters.

Parameter	Abbreviation	Initial	Optimization	Unit
Rotor outer radius	R_1	22.25	21.25	mm
Segmental rotor span	R_2	15	25	mm
Segmental rotor high	R_3	7.25	7.25	mm
Segmental rotor inner radius	*Ri*	15	14	degree
Stator outer radius	*So*	37.5	37.5	mm
Stator inner radius	*Si*	22.5	21.5	mm
Armature slot high	A_1	10	10.4	mm
Armature slot width	A_2	8.65	8.35	mm
FEC slot high	F_1	10	11.4	mm
FEC slot width	F_2	8.65	8.61	mm
Air gap	*Ag*	0.25	0.25	mm

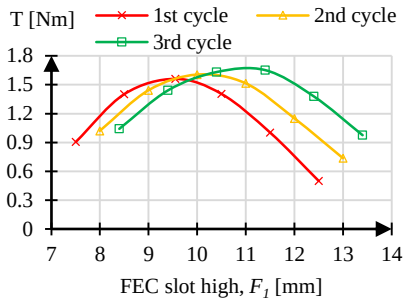

Fig. 11. Torque versus FEC slot high, F_1.

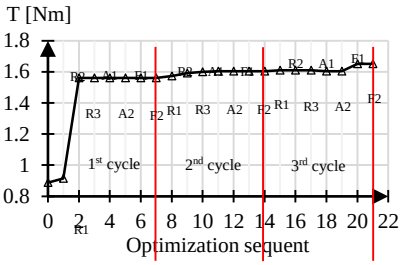

Fig. 12. Torque summary of various motor parameters optimization.

5. Result Comparisons of Preliminary and Optimized Designs

The performance comparison of the proposed FEFSM using segmental rotor is conducted under open-circuit and closed-circuit analyses. The open-circuit analyses incorporate flux linkage, back-emf, and flux line, while the short-circuit analyses consist of torque versus FE current density, J_E at various armature current density, J_A, and torque-power versus speed characteristics.

5.1. Flux linkage

Figure 13 shows the flux linkage comparison between the initial and optimized design of the proposed single-phase FEFSM using a segmental rotor. Clearly, the flux profile of optimized design at maximum J_E is more sinusoidal, and 64% higher than the initial design. In addition, the flux linkage at maximum J_A becomes more balance, in which, the ratio between positive and negative amplitudes has been reduced from 1.7 to 1.15.

The maximum flux for J_A is 0.11 Wb, 35.5% higher than the flux at maximum J_E. Besides, the larger rotor span, R_2 allows flux to flow between two stator teeth and one segmental rotor, hence, in reducing flux leakage and thus, increasing flux linkage as illustrated in Fig. 14.

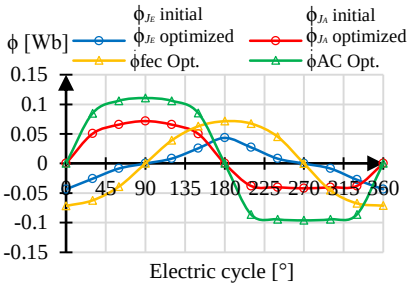

Fig. 13. Result of flux linkage.

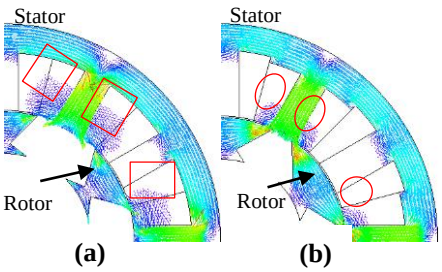

Fig. 14. Flux distribution: (a) initial, (b) optimized designs.

5.2. Back-emf

The back-emf comparison between the initial and optimized design of the proposed motor is depicted in Fig. 15. Both back-emf profiles are taken at the speed of 500 rpm. Figure 15 shows that the highest back-emf amplitude after optimization is 24.9 V, which is 85.7% higher than the initial design. However, the back-emf profile shows a lot of improvement, especially, distortion in 3rd and 5th harmonics have decreased by 78.5% and 84.4%, respectively as illustrated in Fig. 16.

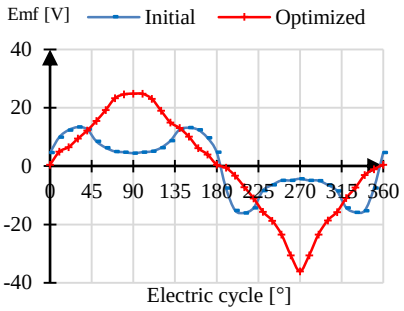

Fig. 15. Result of back-emf.

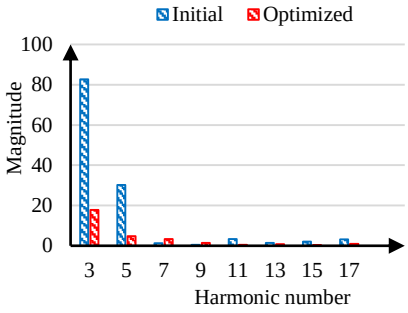

Fig. 16. THD versus harmonic number.

5.3. Flux line

Figure 17 delineates the flux line of the proposed single-phase FEFSM using a segmental rotor, delivered under maximum J_A of 30 A_{rms}/mm^2 at 270° electric cycle. The flux lines in the optimized design indicate a very less flux leakage compared to the initial design. It proves that optimization in R_2 has successfully increased the flux focusing into the flux path and prevented flux leakage occurs to the area of armature coil and FEC slots. As a result, unbalanced flux problems as discussed previously have been resolved and flux enables to flow smoothly to produce high torque.

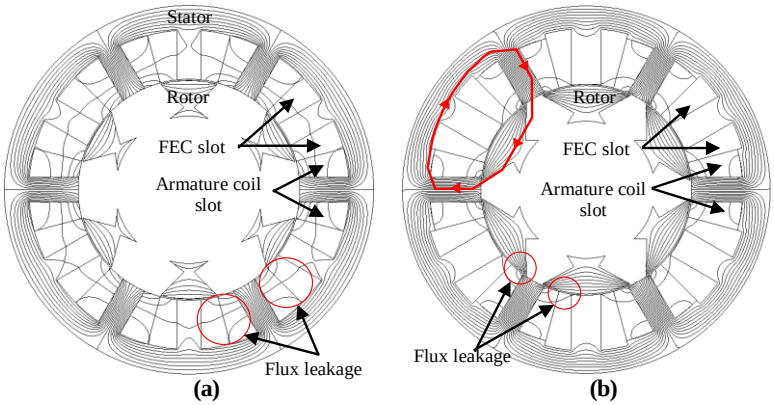

Fig. 17. Flux line of (a) initial, (b) optimized designs.

5.4. Torque at various J_E and J_A

Torque capabilities of the proposed single-phase FEFSM using segmental rotor at various J_E and J_A are demonstrated in Fig. 18. Obviously, the torque increases parallelly with an increase of J_A and J_E. The torque of optimized design has increased by 85.4% from 0.89 Nm to 1.65 Nm obtained at maximum J_A and J_E of 30 A_{rms}/mm^2 and 30 A/mm^2, respectively, proves the optimal torque of optimization processes. In addition, at the maximum J_E of 30 A/mm^2, and J_A of 10 A_{rms}/mm^2 and 20 A_{rms}/mm^2, the highest torque obtained are 0.74 Nm and 1.32 Nm, respectively.

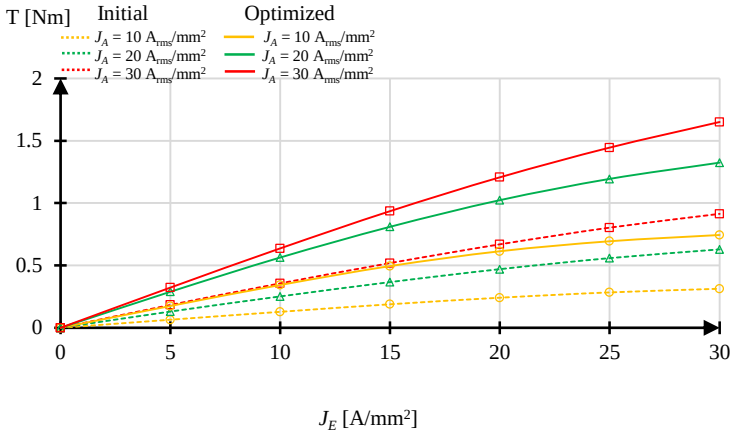

Fig. 18. Torque at various armature current and FEC current densities.

5.5. Torque and power versus speed characteristics

The torque and power versus speed characteristics of the initial and optimized design of the proposed FEFSM using segmental rotor are plotted in Fig. 19. It can be seen that the optimized design has higher torque and power capabilities in the high-speed region compared to the preliminary design. Torque for the optimized design shows the maximum torque constant at the initial stage and start to decline at the speed of 2,304 rpm, while for preliminary design the torque starts to decrease at 2,899 rpm. The power produced from preliminary and optimized designs is 277.5 W and 398.6 W respectively, increased by 43.6%. The summary of performance comparison between preliminary and optimized is illustrated in Table 3.

Table 3. Performance comparison of preliminary and optimized designs.

Parameter	Abbreviation	Initial	Optimization	Unit
Flux linkage	*Φ*	0.0435	0.0714	Wb
Back-emf	*Emf*	13.4	24.9	V
Torque	*T*	0.89	1.65	Nm
Power	*P*	277.4	398.6	W
Based speed	*ns*	2,899	2,304	rpm
Maximum FEC current	*Ia*	10.5	10.5	A
Maximum armature current	*Ie*	7.5	7.5	A
FEC turn	*Ne*	93	93	Turn
Armature coil turn	*Na*	93	93	Turn
Air gap	*Ag*	0.25	0.25	mm

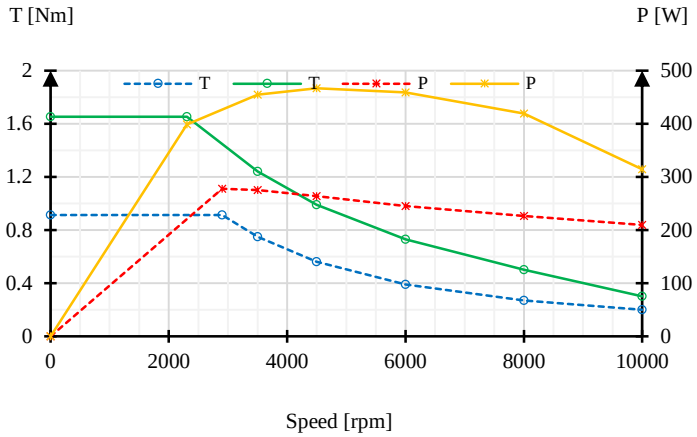

Fig. 19. Torque and power versus speed.

6. Conclusions

This paper has proposed a new single-phase FEFSM using a segmental rotor and non-overlap windings. Preliminary comparisons between FEFSM using salient and segmental rotors indicate that segmental structure has produced shorter flux path and 11 times higher of flux linkage than the salient rotor. The optimization technique has been clearly described and the performance between the initial and optimized designs is compared. As a result, the highest impact in torque improvement has been obtained from the optimization of segmental rotor span (R_2) with an increase of 71.4%. In conclusions, the proposed motor is considered as the best single-phase FEFSM candidates due to the optimized machine design has improved approximately 85.4% and 43.6% of torque and power, respectively from the preliminary design.

Acknowledgements

This research work was under the Fundamental Research Grant Scheme (FRGS), Vot. Number 1651 funded by Ministry of Education Malaysia (MoE) thru Universiti Tun Hussein Onn Malaysia (UTHM).

References

1. Fernando, N.; Nutkani, I.U.; Saha, S.; and Niakinezhad, M. (2017). Flux switching machines : A review on design and applications. *Proceedings of the 20th International Conference on Electrical Machines and Systems (ICEMS). Sydney, New South Wales, Australia*, 1-6.
2. Khan, F.; Sulaiman, E.; and Ahmad, M.Z. (2016). Review of switched flux wound-field machines technology. *IETE Technical Review*, 34(4), 343-352.
3. Nguyen, H.Q.; Jiang, J.-Y.; and Yang, S.-M. (2016). Design of a 12-slot 7-pole wound-field flux switching motor for traction applications. *Proceedings of the IEEE International Conference on Industrial Technology (ICIT). Taipei, Taiwan*, 1275-1280.
4. Ahmad, M.Z.; Sulaiman, E.; Romalan, G.M.; and Haron, Z.A. (2015). Optimal torque investigation of outer-rotor hybrid excitation flux switching machine

for in-wheel drive EV. *ARPN Journal of Engineering Applied Sciences*, 10(19), 8573-8580.

5. Kosaka, T.; Matsui, N.; Kamada, Y.; and Kajiura, H. (2014). Experimental drive performance evaluation of high power density wound field flux switching motor for automotive applications. *Proceedings of the IET International Conference on Power Electronics, Machines and Drives (PEMD)*. Manchester, United Kingdom, 1-6.
6. Sulaiman, E.; Khan, F.; Omar, M.F.; Romalan, G.M.; and Jenal, M. (2016). Optimal design of wound-field flux switching machines for an all-electric boat. *Proceedings of the 22nd International Conference on Electrical Machines (ICEM)*. Lausanne, Switzerland, 2464-2470.
7. Sulaiman, E.; Teridi, M.F M.; Husin, Z.A.; Ahmad, M.Z.; and Kosaka, T. (2013). Performance comparison of 24S-10P and 24S-14P field excitation flux switching machine with single DC-coil polarity. *Proceedings of the 7th International Power Engineering and Optimization Conference (PEOCO)*. *Langkawi, Malaysia*, 46-51.
8. Sulaiman, E.; Kosaka, T.; and Matsui, N. (2012). Design study and experimental analysis of wound field flux switching motor for HEV applications. *Proceedings of the 20th International Conference on Electrical Machine. Marseille, France*, 1269-1275.
9. Tang, Y.; Paulides, J.J.H.; Motoasca, T.E.; and Lomonova, E.A. (2012). Flux-switching machine with DC excitation. *IEEE Transactions on Magnetics*, 48(11), 3583-3586.
10. Chishko, S.D.; Tang, Y.; Paulides J.J.H.; and Lomonova, E.A. (2014). DC excited flux-switching motor: Rotor structural optimization. *Proceedings of the 17th International Conference on Electrical Machines and Systems (ICEMS). Hangzhou, China*, 2867-2871.
11. Khan, F.; Sulaiman, E.; Omar, M.F.; and Jenal, M. (2016). Performance comparison of wound field flux switching machines. *Proceedings of the IEEE Conference on Energy Conversion (CENCON)*. Johor Bahru, Malaysia, 310-314.